

# Overview of Missile Flight Control Systems

*Paul B. Jackson*



*The flight control system is a key element that allows the missile to meet its system performance requirements. The objective of the flight control system is to force the missile to achieve the steering commands developed by the guidance system. The types of steering commands vary depending on the phase of flight and the type of interceptor. For example, in the boost phase the flight control system may be designed to force the missile to track a desired flight-path angle or attitude. In the midcourse and terminal phases the system may be designed to track acceleration commands to effect an intercept of the target. This article explores several aspects of the missile flight control system, including its role in the overall missile system, its subsystems, types of flight control systems, design objectives, and design challenges. Also discussed are some of APL's contributions to the field, which have come primarily through our role as Technical Direction Agent on a variety of Navy missile programs.*

## **INTRODUCTION**

The missile flight control system is one element of the overall homing loop. Figure 1 is a simplified block diagram of the missile homing loop configured for the terminal phase of flight when the missile is approaching intercept with the target. The missile and target motion relative to inertial space can be combined mathematically to obtain the relative motion between the missile and the target. The terminal sensor, typically an RF or IR seeker, measures the angle between an inertial reference and the missile-to-target line-of-sight (LOS) vector,

which is called the LOS angle. The state estimator, e.g., a Kalman filter, uses LOS angle measurements to estimate LOS angle rate and perhaps other quantities such as target acceleration. The state estimates feed a guidance law that develops the flight control commands required to intercept the target. The flight control system forces the missile to track the guidance commands, resulting in the achieved missile motion. The achieved missile motion alters the relative geometry, which then is sensed and used to determine the next set of flight control

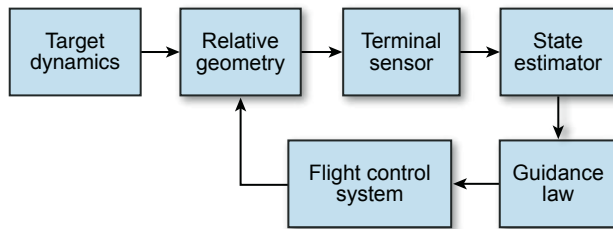


**Figure 1.** The flight control system is one element in the missile homing loop. The inertial missile motion controlled by the flight control system combines with the target motion to form the relative geometry between the missile and target. The terminal sensor measures the missile-to-target LOS angle. The state estimator forms an estimate of the LOS angle rate, which in turn is input to the guidance law. The output of the guidance law is the steering command, typically a translational acceleration. The flight control system uses the missile control effectors, such as aerodynamic tail surfaces, to force the missile to track steering commands to achieve a target intercept.

commands, and so on. This loop continues to operate until the missile intercepts the target.

In the parlance of feedback control, the homing loop is a feedback control system that regulates the LOS angle rate to zero. As such, the overall stability and performance of this control system are determined by the dynamics of each element in the loop. Consequently, the flight control system cannot be designed in a vacuum. Instead, it must be designed in concert with the other elements to meet overall homing-loop performance requirements in the presence of target maneuvers and other disturbances in the system, e.g., terminal sensor noise (not shown in Fig. 1), which can negatively impact missile performance.

The remainder of this article is divided into six sections. The first section discusses the specific elements of the flight control system. Particular emphasis is placed on understanding the dynamics of the missile and how they affect the flight control system designer. The next three sections describe different types of flight control systems, objectives to be considered in their design, and a brief design example. The last two sections discuss some of the challenges that need to be addressed in the future and APL's contributions to Navy systems and the field in general.

## FLIGHT CONTROL SYSTEM ELEMENTS

As noted above, the flight control system is one element of the overall homing loop. Figure 2 shows the basic elements of the flight control system, which itself is another feedback control loop within the overall homing loop depicted in Fig. 1. An inertial measurement unit (IMU) measures the missile translational acceleration and angular velocity. The outputs of the IMU are

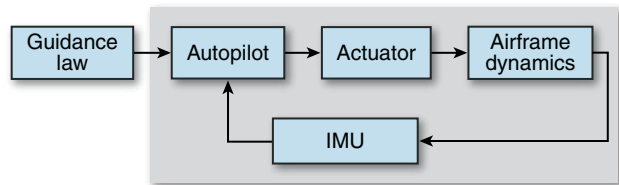


**Figure 2.** The four basic elements of the flight control system are shown in the gray box. The IMU senses the inertial motion of the missile. Its outputs and the inputs from the guidance law are combined in the autopilot to form a command input to the control effector, such as the commanded deflection angle to an aerodynamic control surface. The actuator turns the autopilot command into the physical motion of the control effector, which in turn influences the airframe dynamics to track the guidance command.

combined with the guidance commands in the autopilot to compute the commanded control input, such as a desired tail-surface deflection or thrust-vector angle. An actuator, usually an electromechanical system, forces the physical control input to follow the commanded control input. The airframe dynamics respond to the control input. The basic objective of the flight control system is to force the achieved missile dynamics to track the guidance commands in a well-controlled manner. The figures of merit (FOMs) used to assess how well the flight control system works are discussed in *Flight Control System Design Objectives*. This section provides an overview of each element of the flight control loop.

## Guidance Inputs

The inputs to the flight control system are outputs from the guidance law that need to be followed to ultimately effect a target intercept. The specific form of the flight control system inputs (acceleration commands, attitude commands, etc.) depends on the specific application (discussed later). In general, the flight control system must be designed based on the expected characteristics of the commands, which are determined by the other elements of the homing loop and overall system requirements. Characteristics of concern can be static, dynamic, or both. An example of a static characteristic is the maximum input that the flight control system is expected to be able to track. For instance, a typical rule of thumb for intercepting a target that has constant acceleration perpendicular to the LOS is for the missile to have a 3:1 acceleration advantage over the target. If the missile system is expected to intercept a 10-g accelerating threat, then the flight control system should be able to force the missile to maintain a 30-g acceleration. An example of a dynamic characteristic is the expected frequency content of the command. For instance, rapid changes in the command are expected as the missile approaches intercept against a maneuvering threat, but the input commands may change more slowly during

the midcourse phase of flight where the objective is to keep the missile on an approximate collision path or to minimize energy loss. Other dynamic characteristics of concern include the guidance command update rate and the amount of terminal sensor noise flowing into the flight control system and causing unnecessary control actuator activity.

### Airframe Dynamics

Recall that the objective of the flight control system is to force the missile dynamics to track the input command. The dynamics of the airframe are governed by fundamental equations of motion, with their specific characteristics determined by the missile aerodynamic response, propulsion, and mass properties. Assuming that missile motion is restricted to the vertical plane (typical for early concept development), the equations of motion that govern the missile dynamics can be developed in straightforward fashion.

Consider the diagram in Fig. 3, which shows the missile flying in space constrained to the vertical plane. The angle between the inertial reference axis and the missile velocity vector is called the flight-path angle  $\gamma$ . The angle from the velocity vector to the missile centerline is called the angle of attack (AOA)  $\alpha$ . The angle from the inertial reference to the missile centerline is called the pitch angle  $\theta$ . Acceleration in the direction normal to the missile  $A_z$  derives from two sources. The non-zero AOA generates aerodynamic lift. Normal acceleration

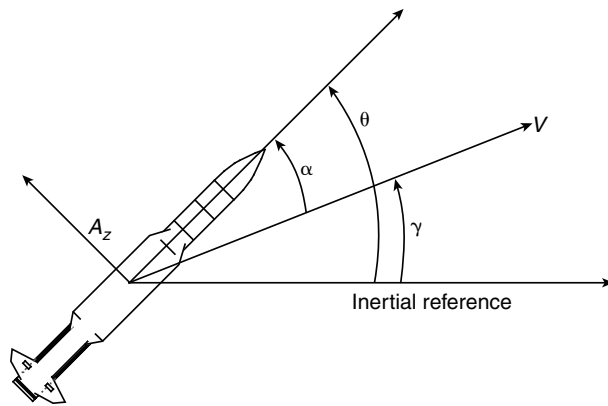


**Figure 3.** In the pitch plane, the missile dynamics and kinematics can be described by four variables.  $A_z$  is the component of the translational acceleration normal to the missile longitudinal axis. The AOA,  $\alpha$ , is a measure of how the missile is oriented relative to the airflow and is the angle between the missile velocity vector and the missile longitudinal axis. The flight-path angle  $\gamma$  is a measure of the direction of travel relative to inertial space, i.e., the angle between the missile velocity vector and an inertial reference. The pitch angle  $\theta$  defines the missile orientation relative to inertial space and is the angle between the inertial reference and the missile longitudinal axis.

also can be developed by a control input  $\delta$  such as tail-fin deflection or thrust-deflection angle. In general, the missile acceleration also has a component along the centerline due to thrust and drag. For the simple model being developed here, we assume that this acceleration is negligible.

Based on the diagram in Fig. 3, the fundamental relationship among the three angles above is

$$\alpha = \theta - \gamma \rightarrow \dot{\alpha} = \dot{\theta} - \dot{\gamma}. \quad (1)$$

The angular acceleration is the moment applied to the airframe divided by the moment of inertia,

$$\ddot{\theta} = \frac{M(\alpha, \delta)}{J}. \quad (2)$$

The applied moment is a function of the control input  $\delta$  and the aerodynamic force induced by the AOA. The rate of change of the flight-path angle is the component of missile acceleration perpendicular to the velocity vector divided by the magnitude of the velocity vector. Assuming that the AOA is small, the flight-path angle rate is

$$\dot{\gamma} = \frac{A_z \cos(\alpha)}{V} \approx \frac{A_z}{V}. \quad (3)$$

The normal acceleration is determined by the forces applied to the missile divided by its mass

$$A_z = \frac{F_z(\alpha, \delta)}{m}. \quad (4)$$

The applied force is a function of the control input  $\delta$  and the aerodynamic force induced by the AOA. Substituting Eqs. 3 and 4 into Eq. 1 and combining the result with Eq. 2 yields a coupled set of nonlinear differential equations where the state variables are the AOA and the pitch rate:

$$\begin{aligned} \dot{\alpha} &= \dot{\theta} - \frac{F_z(\alpha, \delta)}{mV} \\ \ddot{\theta} &= \frac{M(\alpha, \delta)}{J}. \end{aligned} \quad (5)$$

Although these differential equations can be solved numerically, an analytical approach often is desirable to fully understand the missile dynamics. Therefore, the equations of motion are linearized around an operating condition so that linear systems theory can be applied. Assuming constant missile speed, linearization of Eq. 5 yields a second-order state-space description of the missile dynamics

$$\begin{bmatrix} \dot{\alpha} \\ \ddot{\theta} \end{bmatrix} = \underbrace{\begin{bmatrix} -\frac{Z_\alpha}{V} & 1 \\ M_\alpha & 0 \end{bmatrix}}_A \begin{bmatrix} \alpha \\ \dot{\theta} \end{bmatrix} + \underbrace{\begin{bmatrix} -\frac{Z_\delta}{V} \\ M_\delta \end{bmatrix}}_B \delta \quad (6)$$

$$\begin{bmatrix} \dot{\theta} \\ A_z \end{bmatrix} = \underbrace{\begin{bmatrix} 0 & 1 \\ Z_\alpha & 0 \end{bmatrix}}_C \begin{bmatrix} \alpha \\ \dot{\theta} \end{bmatrix} + \underbrace{\begin{bmatrix} 0 \\ Z_\delta \end{bmatrix}}_D \delta,$$

where the numerical coefficients are defined by

$$\begin{aligned} Z_\alpha &= \frac{1}{m} \frac{\partial F_z(\alpha, \delta)}{\partial \alpha} \\ Z_\delta &= \frac{1}{m} \frac{\partial F_z(\alpha, \delta)}{\partial \delta} \\ M_\alpha &= \frac{1}{J} \frac{\partial M(\alpha, \delta)}{\partial \alpha} \\ M_\delta &= \frac{1}{J} \frac{\partial M(\alpha, \delta)}{\partial \delta} \end{aligned} \quad (7)$$

and are evaluated at the particular operating condition of interest. Because these differential equations result from linearization around an operating point, the state, input, and output variables actually represent small signal perturbations around that operating point.

These linear differential equations apply for any missile under the stated assumptions. However, specific dynamics governed by these equations differ depending on the application. For example, for a tail-controlled endoatmospheric interceptor, the dynamics are a weak function of  $Z_\delta$ . For a thrust-vector-controlled exoatmospheric interceptor, the aerodynamic forces are negligible and the terms  $Z_\alpha$  and  $M_\alpha$  can be set to zero.

The linear differential equations determine the dynamic behavior of the missile for small perturbations around the specified operating conditions. For example, suppose the missile is given an initial condition at an AOA a few degrees away from the nominal AOA around which the dynamics have been linearized. One important question is whether the missile will rotate back to the nominal AOA or diverge in the absence of any corrective control input. The answer to this question of stability is determined by the roots of the characteristic polynomial of the state matrix in Eq. 6:

$$s^2 + \frac{Z_\alpha}{V} s + (-M_\alpha) = 0. \quad (8)$$

A necessary and sufficient condition for both roots of this equation to have negative real parts and thus ensure stability is that all of the coefficients be positive. Using the conventions in Fig. 3,  $Z_\alpha$  is always positive. Therefore, the stability of the missile in the absence of a control input is determined by the sign of  $M_\alpha$ . If  $M_\alpha$  is

positive, the aerodynamic pitching moment forces the missile to diverge from the nominal AOA, and the missile is said to be statically unstable. If  $M_\alpha$  is negative, the missile tends to be restored back to the nominal AOA, and the missile is said to be statically stable. The static stability of the missile is a crucial property that, under the stated assumptions, is determined solely by the sign of  $M_\alpha$ , which is in turn determined by the aerodynamic configuration and the location of the missile center of mass.

Figure 4 illustrates in the complex s-plane how the roots of the characteristic equation migrate as a function of  $M_\alpha$ . Again, for large, positive values of  $M_\alpha$ , the missile is statically unstable, and the dynamics are governed by one unstable real root in the right half of the plane and one stable real root in the left half of the plane. As  $M_\alpha$  decreases, the roots migrate toward the origin. When  $M_\alpha$  is zero, the system has one real, stable root in the left half plane and one root at the origin. This condition is called neutral stability. As  $M_\alpha$  becomes more negative, the roots migrate toward each other and eventually split apart as a complex pair.

The state-space representation in Eq. 6 describes the missile dynamics in the time domain. A representation in the complex frequency domain can be obtained that relates the input to the system, e.g., tail-deflection angle, to the system outputs, e.g., pitch rate and normal acceleration. This type of representation is called the trans-

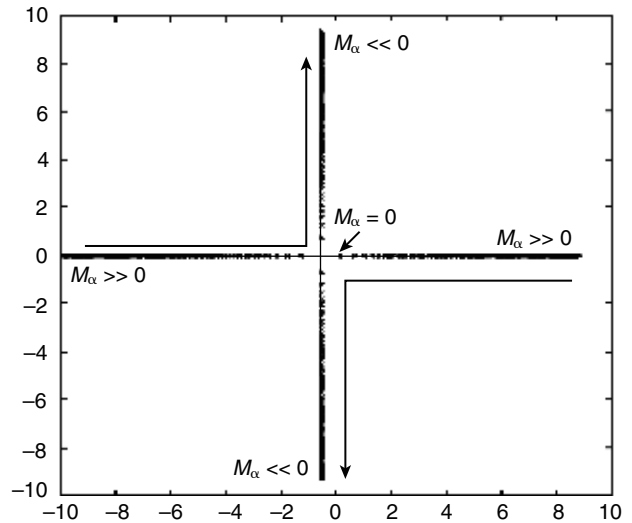


**Figure 4.** Static stability of the airframe is determined by the slope of the pitching moment curve with respect to the AOA,  $M_\alpha$ . If the slope is positive, the missile is statically unstable because one of the roots of the characteristic polynomial of the governing differential equation is in the right half of the complex plane. If the slope is negative, both roots are in the left half of the plane and the missile is statically stable. The case where the slope is zero is called neutral stability, with one of the roots at the origin of the complex plane.

fer function and can be determined from the state-space model using the formula

$$H(s) = C(sI - A)^{-1}B + D, \quad (9)$$

where  $s = \sigma + j\omega$  is complex frequency and  $A$ ,  $B$ ,  $C$ , and  $D$  are defined in Eq. 6.

In reality, missiles are not constrained to motion in a single plane. Figure 5 shows the relevant variables that describe the missile kinematics in three dimensions. The angle of sideslip (AOS)  $\beta$  is the yaw equivalent to the AOA. Together, they completely specify how the missile body is oriented relative to its velocity vector. The three components of the missile body angular velocity vector resolved in body-fixed coordinates are denoted  $p$ ,  $q$ , and  $r$ , denoting the roll, pitch, and yaw rate, respectively. The pitch rate  $q$  was denoted as  $\dot{\theta}$  in the discussion above where the motion was constrained to the pitch plane.

The equations that govern the dynamics of the missile can be developed by applying the Newton–Euler equations of motion. The

translational motion can be described in terms of the derivatives of the AOA and the AOS. The rotational motion can be described in terms of the angular accelerations and takes a simple form assuming that products of inertia are zero:

$$\begin{aligned} \dot{\alpha} &= \cos^2\alpha \left( \frac{F_{zb}}{mu} - p \tan\beta + q \sec^2\alpha - \frac{F_{xb}}{mu} \tan\alpha - r \tan\alpha \tan\beta \right) \\ \dot{\beta} &= \cos^2\beta \left( \frac{F_{yb}}{mu} - r \sec^2\beta + p \tan\alpha - \frac{F_{xb}}{mu} \tan\beta + q \tan\alpha \tan\beta \right) \end{aligned} \quad (10)$$

$$\begin{aligned} \dot{p} &= \frac{M_{xb}}{I_x} - \frac{I_z - I_y}{I_x} qr \\ \dot{q} &= \frac{M_{yb}}{I_y} - \frac{I_x - I_z}{I_y} pr \\ \dot{r} &= \frac{M_{zb}}{I_z} - \frac{I_y - I_x}{I_z} pq. \end{aligned} \quad (11)$$

The lateral components of missile inertial translational acceleration resolved in body-fixed coordinates are

$$\begin{aligned} A_z &= \frac{F_{zb}}{m} \\ A_y &= \frac{F_{yb}}{m}. \end{aligned} \quad (12)$$

In these equations the forces and moments are resolved in body coordinates, with components indicated by the subscripts. Though not shown explicitly, all of the six components of the force and moment vectors are functions of the state variables and three control inputs, e.g.,

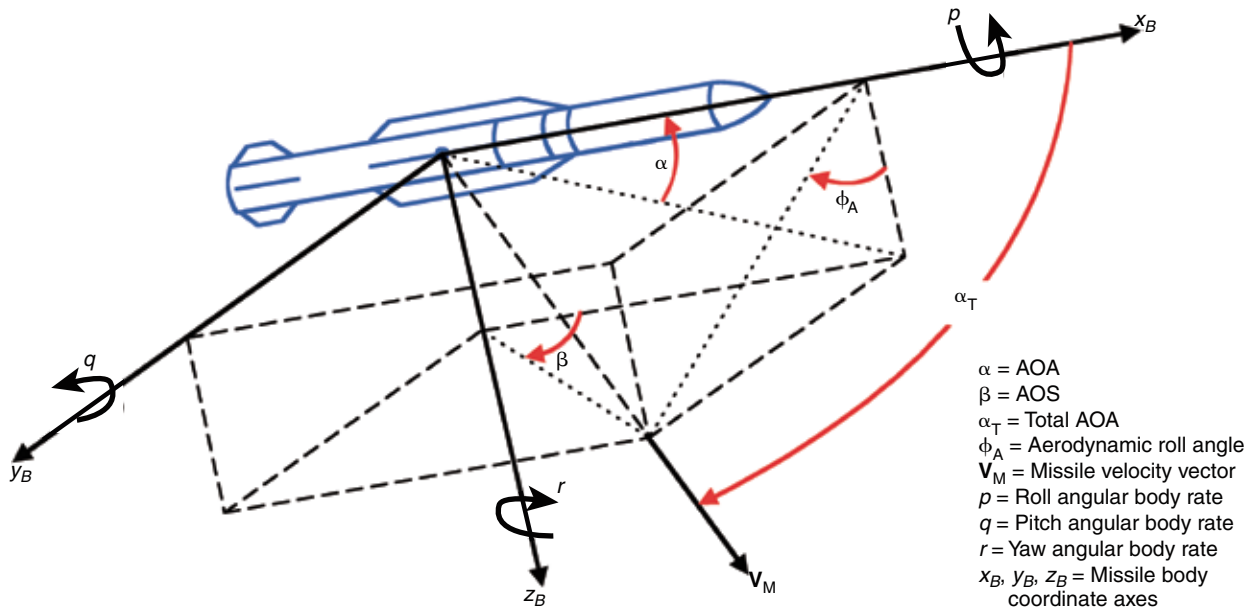


**Figure 5.** This diagram defines quantities used to describe the three-dimensional missile kinematics. Two angles are used to orient the missile relative to the velocity vector, either AOA and AOS or total AOA and aerodynamic roll angle. The components of the missile inertial velocity vector resolved in body-fixed axes are  $u$ ,  $v$ , and  $w$  (not shown). The components of the inertial angular velocity vector resolved in body-fixed coordinates are  $p$ ,  $q$ , and  $r$ . The missile orientation in inertial space usually is described via three Euler angles, typically in yaw–pitch–roll sequence (not shown).

$$F_{zb} = f(\alpha, \beta, p, q, r, \delta_p, \delta_y, \delta_r). \quad (13)$$

The dynamic equations together are a coupled, fifth-order, nonlinear differential equation. In situations where the mass properties vary with time, such as when a rocket motor is burning propellant, the differential equation is time-varying as well.

Equations 10–12 can be linearized around some operating condition of interest by expanding them in a Taylor series and retaining only the first-order terms. The result is a linear, time-invariant, state-space model with three inputs and five outputs:

$$\begin{aligned} \dot{x} &= Ax + Bu \\ y &= Cx + Du \\ x &= [\alpha \quad \beta \quad p \quad q \quad r]^T \\ u &= [\delta_p \quad \delta_y \quad \delta_r]^T \\ y &= [A_y \quad A_z \quad p \quad q \quad r]^T. \end{aligned} \quad (14)$$

As in the planar case, the state variables, control input variables, and output variables represent perturbations around the nominal operating condition.

Expanding the model to account for yaw and roll in addition to pitch brings a new set of challenges to the flight control designer. Foremost among these in many applications is aerodynamic cross-coupling as the total AOA increases, in which case aerodynamic surfaces on the leeward side of the missile become shaded by the fuselage, resulting in aerodynamic imbalances. The net effect typically results in undesirable motion, such as roll moment induced by a change in AOA or pitch moment induced by roll control input. The flight control system must compensate for these effects. An alternative is to simplify the airframe design to minimize cross-coupling, but the airframe must be designed with other factors in mind as well, such as maximizing the effective range of the missile. Compensating for aerodynamic cross-coupling for some missiles is challenging and often limits the maximum total AOA, and hence the maximum lateral acceleration, that can be achieved by the flight control system.

## Actuator

The missile actuator converts the desired control command developed by the autopilot into physical motion, such as rotation of a tail fin, that will effect the desired missile motion. Actuators for endoatmospheric missiles typically need to be high-bandwidth devices (significantly higher than the desired bandwidth of the flight control loop itself) that can overcome significant loads. Most actuators are electromechanical, with hydraulic actuators being an option in certain applications. For early design and analysis, the actuator

dynamics are modeled with a second-order transfer function (which does not do justice to the actual complexity of the underlying hardware),

$$\frac{\delta(s)}{\delta_c(s)} = \frac{\omega_a^2}{s^2 + 2\zeta_a \omega_a s + \omega_a^2}. \quad (15)$$

Although the actuator often is modeled as a linear system for preliminary design and development, it is actually a nonlinear device, and care must be taken by the flight control designer not to exceed the hardware capabilities. Two critical FOMs for the actuator for many endoatmospheric missiles are its rate and position limits. The position limit is an effective limit on the moment that the control input can impart on the airframe, which in turn limits the maximum AOA and acceleration. The rate limit essentially limits how fast the actuator can cause the missile to rotate, which effectively limits how fast the flight control system can respond to changes in the guidance command. The performance of a flight control system that commands the actuator to exceed its limits can be degraded, particularly if the missile is flying at a condition where it is statically unstable.

## Inertial Measurement Unit

The IMU measures the missile dynamics for feedback to the autopilot. In most flight control applications, the IMU is composed of accelerometers and gyroscopes to measure three components of the missile translational acceleration and three components of missile angular velocity. For early design and analysis, the IMU dynamics often are represented by a second-order transfer function,

$$\frac{y_m(s)}{y(s)} = \frac{\omega_m^2}{s^2 + 2\zeta_m \omega_m s + \omega_m^2}, \quad (16)$$

for each rate and acceleration channel. Like the actuator, the IMU needs to be a high-bandwidth device relative to the desired bandwidth of the flight control loop. In some applications, other quantities also need to be measured, such as the pitch angle for an attitude control system. In this case, other sensors can be used (e.g., an inertially stabilized platform), or IMU outputs can feed strapdown navigation equations that are implemented in a digital computer to determine the missile attitude, which then is sent to the autopilot as a feedback measurement.

The flight control system must be designed such that the missile dynamics do not exceed the dynamic range of the IMU. If the IMU saturates, the missile will lose its inertial reference, and the flight control feedback is corrupted. The former may be crucial, depending on the specific missile application and the phase of flight. The

latter may be more problematic if the dynamic range is exceeded for too long, particularly if the missile is statically unstable.

## Autopilot

The autopilot is a set of equations that takes as inputs the guidance commands and the feedback measurements from the IMU and computes the control command as the output. As mentioned previously, the autopilot must be designed so that the control command does not cause oversaturation of the actuator or the IMU. Because the autopilot usually is a set of differential equations, computing its output involves integrating signals with respect to time. Most modern autopilots are implemented in discrete time on digital computers, although analog autopilots are still used. The following section describes several types of autopilots that apply in different flight control applications.

## TYPES OF FLIGHT CONTROL SYSTEMS

The specific type of flight control system that is implemented on a particular missile depends on several factors, including the overall system mission and requirements, packaging constraints, and cost. In many applications, the type of flight control system changes with different phases of flight. For example, the system used during the boost phase for a ground- or ship-launched missile could very well differ from the system used during the intercept phase. This section provides a brief overview of different types of flight control systems and when they might be used.

### Acceleration Control System

One type of flight control system common in many endoatmospheric applications is designed to track commanded acceleration perpendicular to the missile longitudinal axis. In this system, deflection of an aerodynamic

control surface, such as a tail fin, is the control input, and pitch angular rate ( $q$ ) and acceleration ( $A_z$ ) are measured by the IMU for feedback to the autopilot. The control deflection produces a small aerodynamic force on the tail fin but a large moment on the airframe because of its lever arm from the center of mass. The induced moment rotates the missile to produce the AOA, which in turn produces aerodynamic lift to accelerate the airframe.

Figure 6 represents equations that can be implemented in the autopilot to develop the commanded control surface deflection angle  $\delta$  based on the commanded acceleration and feedback measurements of achieved acceleration  $A_z$  and pitch rate  $q$ . This particular structure can be found in many missile applications, but is by no means exclusive. As indicated in Fig. 6, the error between the commanded and achieved acceleration is used as an input to the inner control loops that control missile pitch rate. The pitch rate control loops include integration with respect to time that is implemented in circuitry for an analog autopilot or with numerical difference equations in a computer in a digital autopilot. The three control gains are selected so that the closed-loop flight control system has the desired speed of response and robustness consistent with other design constraints such as actuator limits. The autopilot in Fig. 6 is a reasonable starting point for a preliminary design. The final implementation would need to include other features, such as additional filters to attenuate IMU noise and missile vibrations, so that the system would actually work in flight and not just on paper.

### Attitude Control System

Figure 7 shows another type of autopilot that can be used to control the attitude of the missile. In this case, the control effector is the thrust-deflection angle that is actuated by either a nozzle or jet tabs. The feedback loops have a structure similar to that used in the acceleration control system of Fig. 6, except that the outer loop is pitch-angle feedback instead of accelera-

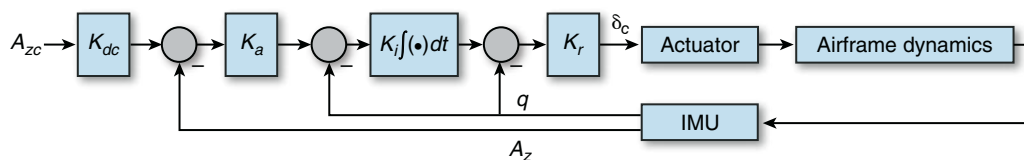


**Figure 6.** This block diagram illustrates a classical approach to the design of an acceleration control autopilot. The difference between the scaled input acceleration command and the measured acceleration is multiplied by a gain to effectively form a pitch rate command. The difference between the effective pitch rate command and the measured pitch rate is multiplied by a gain and integrated with respect to time. The resulting integral is differenced with the measured pitch rate and multiplied by a third gain to form the control effector command such as desired tail-deflection angle. The gain on the input acceleration command ensures zero steady-state error to constant acceleration command inputs. The final autopilot design would build on this basic structure with the addition of noise filters and other features such as actuator command limits. This basic structure is called the three-loop autopilot.

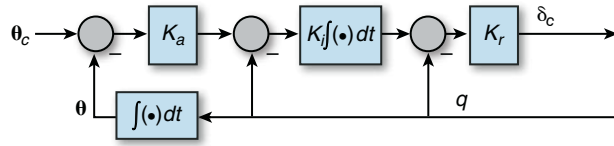


**Figure 7.** This attitude control system also has a three-loop structure like the acceleration control system. The difference lies in the selection of the numerical values of the gains to reflect a different design criterion, i.e., controlling attitude instead of acceleration.

tion. The numerical values of the gains in the control loops may differ for controlling attitude compared to controlling translational acceleration. The integration of pitch rate measured by the IMU to pitch attitude would typically be done via discrete integration in the missile navigation processing in the flight computer.

### Flight-Path Angle Control System

Figure 8 shows an autopilot that can be used to track flight-path angle commands using thrust-vector control. This type of system assumes that aerodynamic forces are small and hence applies for exoatmospheric flight or for endoatmospheric flight when the missile speed is low. In this design, the feedback loops reflect the underlying physical relationships among the flight-path angle, AOA, flight-path angle rate, and pitch rate. The design explicitly uses estimates of the missile thrust and mass properties to compensate for how the missile dynamics change as propellant is expended. The commanded input into the autopilot is the desired flight-path angle. The output is the thrust-vector deflection angle. The feedback signals are the pitch rate  $q$ , flight-path angle rate  $\dot{\gamma}$ , AOA  $\alpha$ , and flight-path angle  $\gamma$ . The pitch rate is measured by the IMU. The other feedback quantities are estimated in the missile navigation processing in the flight computer. This design is an example of the dynamic inversion design approach, which will be discussed in *Technology Development*.

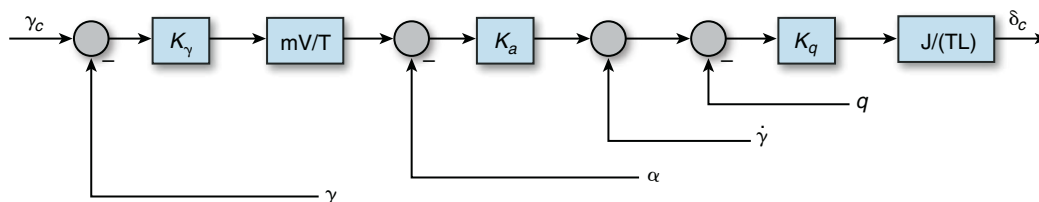


**Figure 8.** This diagram of a flight-path control system shows the dynamic inversion design approach. The design explicitly uses the fundamental relationships among the missile kinematic and dynamic variables as well as real-time estimates of the missile thrust and mass properties to naturally compensate for the changing missile dynamics as propellant is expended.

## FLIGHT CONTROL SYSTEM DESIGN OBJECTIVES

The particular FOMs used to evaluate the flight control system are application dependent. In this section, we explore typical FOMs that would generally apply. A specific application may include others as well.

### Time-Domain Design Objectives

Flight control system FOMs can be expressed in the time and frequency domains. Figure 9 illustrates typical FOMs in the time domain. The plot shows the time response of the missile dynamics in response to a step change in commanded input. For example, this response could represent the achieved missile acceleration in response to a step change in commanded missile acceleration. The time constant and rise time characterize how quickly the system responds to the change in the command. The percentage overshoot and peak amplitude characterize the degree to which the response is well controlled. The steady-state error and settling time are indicators of how well the system tracks the desired command. As might be expected, designing the flight control system can require trade-offs between these FOMs. For example, a system that requires a small time constant may have to suffer larger overshoot.

In addition to time-domain requirements that measure how well the missile tracks the command in the desired plane of motion, the flight control system must be designed to minimize undesirable motion in response to that same command. For example, the missile should minimize motion in the horizontal plane in response to a guidance command in the vertical plane. In other words, the flight control system should “decouple the airframe,” i.e., compensate for the natural aerodynamic coupling specific to the particular airframe in question. Decoupling is important insofar as the derivation of terminal guidance laws assumes a perfectly decoupled flight control system.

### Frequency-Domain Design Objectives

Frequency-domain requirements are based on the classical control theory of Nyquist and Bode and are

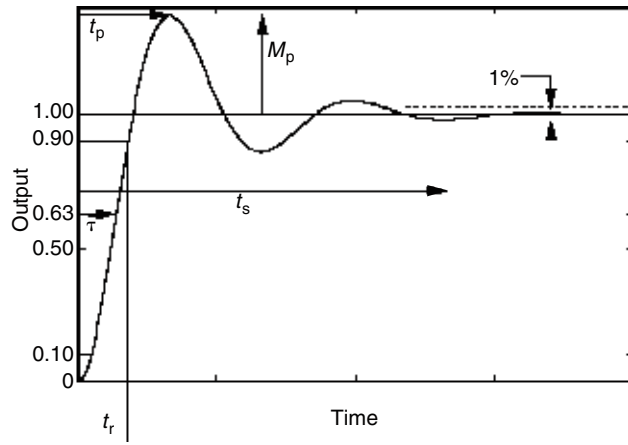


**Figure 9.** Some basic FOMs of a flight control system that are measured in the time domain are illustrated. These FOMs define how quickly the missile will respond to a change in guidance command and also the deviation of the achieved missile motion relative to the command ( $\tau$  is time constant,  $M_p$  is peak magnitude,  $t_p$  is time to first peak,  $t_r$  is rise time, and  $t_s$  is settling time).

primarily concerned with quantifying the robustness of the flight control system. Robustness is important because the flight control system is designed based on models of the missile dynamics, actuator, and IMU, which are inherently approximations (i.e., no model is perfect). Qualitatively, robustness is the degree to which the flight control system can tolerate the error between the assumed models and the real system. Robustness can be addressed in several ways, two of which are discussed below. Classical stability margins quantify how much error can be tolerated at a single point in the system. More advanced techniques can be used to quantify robustness to simultaneous variations to multiple parameters in the model.

**Classical Stability Margins**

Two common measures of robustness are gain and phase margins as determined by an open-loop frequency response computed at a specific point of interest in the system. The open-loop frequency response is computed by breaking the loop at the point of interest and computing the frequency response of the negative of the transfer function from the resulting input to the resulting output (Fig. 10). The gain and phase as a function of frequency often

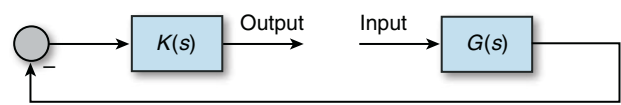


**Figure 10.** The open-loop transfer function at some point of interest is computed by “breaking the loop” at that point and computing the negative of the transfer function from the resulting input to the output. This open-loop transfer function is the bedrock of classical stability analysis in the frequency domain.

are plotted separately on what is called a Bode plot. Figure 11 is a Bode plot of an example open-loop frequency response for an acceleration control system with the loop broken at the input to the actuator. The gain margin is determined from the gain curve at the frequency where the phase crosses 180°. The gain margin tells how much the gain can be increased or decreased at the loop breakpoint before the closed-loop system becomes unstable. The phase margin is determined from the phase curve at the frequency where the gain curve crosses 0 dB. The phase margin tells how much extra phase lag, i.e., delay, can be tolerated at the loop breakpoint before the closed-loop system becomes unstable. Common requirements for gain and phase margins are 6 dB and 30°, respectively.

Mathematically, gain and phase margins only apply at the specific point for which they were computed. From an engineering standpoint, gain and phase variations need to be tolerated at many different points in the system. Qualitatively, the engineer needs to under-

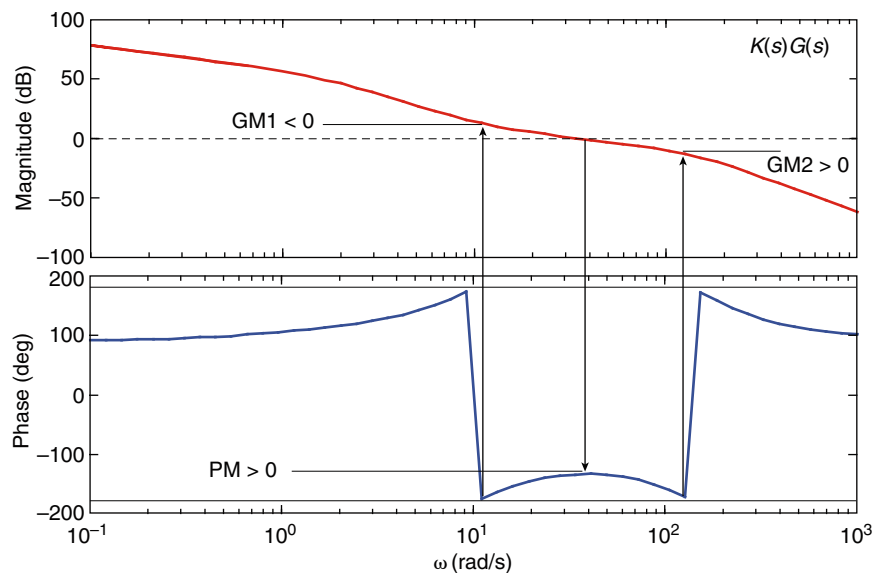


**Figure 11.** This Bode plot shows the open-loop frequency response of an acceleration autopilot with the loop broken at the input to the actuator. In this example, the missile is statically unstable, which results in the phase curve crossing the 180° line twice. The low-frequency crossover yields a decreasing gain margin (GM) and the high-frequency crossover yields an increasing GM. The gain curve crosses the 0-dB line between the phase crossover frequencies, resulting in a positive phase margin (PM). At high frequencies, the monotonically decreasing gain provides robustness to high-frequency modeling errors, uncertainty, and other effects.

stand how all of these variations can be translated to and combined at a single point. Consequently, designing for good gain and phase margins at a single point is an attempt to cover the net effect of all of the variability in the missile that the flight control system must tolerate. Typically, gain and phase margins are computed at the input to the actuator and also should be computed at the outputs of the IMU. In addition, gain and phase margins can be computed at other points in the system that may be of particular interest. For example, it may be useful to know how much  $M_\alpha$  can be increased from its modeled value before the system becomes unstable.

The open-loop frequency response at the actuator shown in Fig. 11 exhibits characteristics common to a good design. At low frequencies, the gain is high, which is required for good command tracking, robustness to low-frequency variations from the modeled system dynamics, and rejection of low-frequency disturbances (e.g., a wind gust or a transient induced by a staging event). At high frequency, the gain is small and decreasing, which provides attenuation of high-frequency disturbances such as sensor noise and robustness to high-frequency variations to the modeled system dynamics, as discussed next.

At higher frequencies, the concept of gain and phase margins applies mathematically but is not as useful realistically because the models used for the design and analysis typically become increasingly inaccurate with increasing frequency because of the fundamental nonlinear nature of the system. Actuators, in particular, do not behave as linear systems at high frequency because of nonlinearities such as friction and backlash. Another issue is that missiles are not perfectly rigid. High-frequency flexible body vibrations in response to actuator motion can be sensed by the IMU and become a destabilizing effect. The net result is that predicted gain and phase values at high frequency can differ considerably from their actual values. A common approach to address this problem is to ensure that the open-loop gain is below some desired value at all frequencies above some certain lower bound. This approach desensitizes the system to high-frequency phase variations. The gain requirement is set based on assumptions about the high-frequency modeling errors, sometimes based on test data, and often comes from hard-learned experience. In general, the less the designer knows about the actual response of the system (relative to the modeled response), the more conservatism must be built into the design.

Not surprisingly, such conservatism comes at a cost. Gain and phase of a linear system across all frequencies must satisfy certain mathematical relationships and cannot be controlled independently. Therefore, the designer cannot decrease the gain at high frequency without also reducing the phase at lower frequencies, which then reduces the phase margin. Phase margin can be recovered by modifying the gain to move the 0-dB

crossover point to lower frequencies, but this in turn will likely slow down the step response and increase the time constant. Conflicts between high-frequency attenuation requirements and low-frequency bandwidth requirements are not uncommon for a high-performance system, particularly with an unstable airframe, and can only be solved by giving up one for the other or re-addressing overall system requirements and the system configuration through systems engineering.

### Robustness to Parameter Variations

So far the concept of robustness has been addressed through gain and phase margins, which apply at a single point or can be loosely thought of as “covering” simultaneous variations, and high-frequency attenuation, which covers high-frequency modeling errors and uncertainty. Another type of robustness that can be useful to quantify is tolerance to specific simultaneous parameter variations in the missile dynamics model, which is a more accurate error model than assuming that only one parameter can vary while holding the others fixed. For example, we might wish to know how much variability can be tolerated in  $M_\alpha$  and  $M_\delta$  simultaneously before the system becomes unstable.

This type of problem can be addressed by realizing that it can be viewed within the framework of Fig. 12. In Fig. 12, the transfer function matrix  $M(s)$  represents the nominal, closed-loop flight control system, where  $w$  represents the guidance command (e.g., commanded acceleration), and  $z$  represents the achieved missile dynamics (e.g., achieved missile acceleration). The feedback matrix  $\Delta$  represents the perturbation to the nominal system. In this example,  $\Delta$  is a  $2 \times 2$  diagonal matrix, with the diagonal elements representing the perturbations to the nominal values of  $M_\alpha$  and  $M_\delta$ . From the diagram, it is apparent that perturbations to the nominal system essentially act as an extra feedback loop. Hence, the question: *How big can  $\Delta$  be before the feedback loop becomes unstable?*

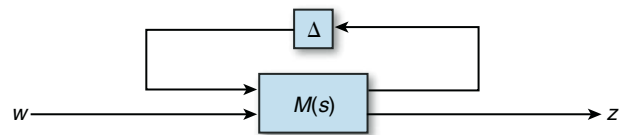


**Figure 12.** This block diagram illustrates a general way to represent the effect of modeling errors or uncertainty in a control system. Here,  $w$  represents the system input (e.g., an acceleration command),  $z$  is the system output (e.g., achieved acceleration),  $M(s)$  is the transfer function model of the nominal system, and  $\Delta$  represents perturbations to the nominal parameters (e.g., moment of inertia or aerodynamic coefficients). The model uncertainty can be represented as the gain in a feedback loop around the nominal system. Because it is a feedback loop, stability of this system can be analyzed using feedback control theory.

One approach to answering this question is illustrated in Fig. 13. Conceptually, a stability boundary is defined by a locus of points in the  $\Delta M_\alpha$ - $\Delta M_\delta$  plane. The goal is to find the minimum distance from the origin to the stability boundary. This constrained minimum distance problem can be solved numerically via a gradient projection search.<sup>1</sup> As with any gradient search, the problem of finding local minima must be addressed. This approach extends to problems of higher order, where the problem is to find the minimum distance from the origin of the perturbation space to an  $n$ -dimensional surface that defines the stability boundary.

Because the perturbations are really a feedback loop around the nominal system, another approach to addressing the simultaneous perturbation problem follows directly from stability theory for multi-input, multi-output feedback control systems. Using the maximum singular value  $\bar{\sigma}$  for the measure of the magnitude of a matrix, the stability problem then is

$$\min_{\Delta}(\bar{\sigma}(\Delta) \mid \text{s.t. system is unstable}), \quad (17)$$

i.e., find the smallest perturbation matrix that destabilizes the system. The solution to this problem follows from the multivariable Nyquist stability theorem and actually is easily solved, assuming that the perturbation matrix  $\Delta$  is a fully populated, complex matrix, when in reality it is a real, diagonal matrix. Hence, this approach tends to be conservative. In practice, much of the conservatism can be reduced by specifying in the minimiza-

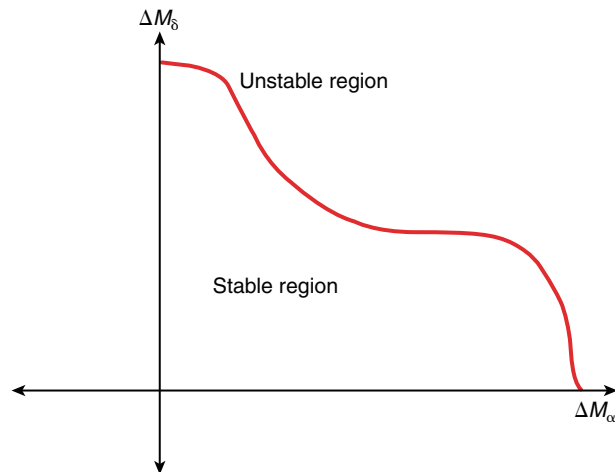


**Figure 13.** The stability of the perturbed system can be represented by regions in the perturbation plane. The analysis problem then is to define the stability boundary and the shortest distance from it to the origin. This problem can be solved with a projected gradient search. This solution approach extends to more than two perturbations and can even be used with complex perturbations that represent changes in both gain and phase at critical points in the system.

tion problem that the perturbation matrix has a specific structure

$$\min_{\Delta}(\bar{\sigma}(\Delta) \mid \text{s.t. system is unstable}, \quad (18)$$

$$\Delta \in \{\text{diagonal matrices}\}.$$

The additional constraint on the structure of the perturbation matrix makes this a much more difficult problem to solve.

Although the simultaneous perturbation problem can be solved mathematically, the flight control engineer still needs to formulate the problem in a meaningful way, particularly when dealing with perturbations to parameters that can have very different dynamic ranges or even different physical units. Hence, determining the appropriate scaling on the perturbed parameters is an important first step in these types of problems.

## PITCH ACCELERATION AUTOPILOT EXAMPLE

This section presents an example of a pitch acceleration autopilot design for a tail-controlled missile and illustrates some of the FOMs discussed above.

The missile dynamics have been linearized around a nominal operating condition of a  $10^\circ$  AOA and a missile speed of Mach 3. Evaluating the slopes in Eq. 7, inserting them into the state-space model, and computing the transfer functions in the frequency domain yields

$$\frac{A_z(s)}{\delta(s)} = \frac{0.2038(s^2 - 34.3^2)}{s + 0.56 \pm 9.32j} \quad (19)$$

$$\frac{q(s)}{\delta(s)} = \frac{-131(s+1)}{s + 0.56 \pm 9.32j}.$$

The denominator of these transfer functions is the same as the left-hand side of the characteristic equation in Eq. 8. At this condition, the missile has a stable airframe with a pair of lightly damped complex poles.

This example assumes that the tail-fin actuator dynamics can be represented by a second-order transfer function (e.g., Eq. 15) with  $\omega_a = 150$  rad/s and  $\zeta_a = 0.7$ . The IMU is assumed to be ideal, i.e., the feedback measurements are equal to their corresponding true values.

The autopilot for this example is the basic three-loop autopilot shown in Fig. 6. The autopilot gains are selected to provide a time constant of less than 0.2 s with minimal overshoot. The resulting autopilot gains are  $K_{dc} = 1.1$ ,  $K_a = 4.5$ ,  $K_i = 14.3$ , and  $K_r = -0.37$ .

The achieved missile acceleration in response to a unit-step acceleration command input is shown in Fig. 14. The time constant is approximately 0.18 s, and the overshoot is only a few percent. The response in Fig. 14 shows that the initial acceleration develops in the negative direction before reversing and eventually

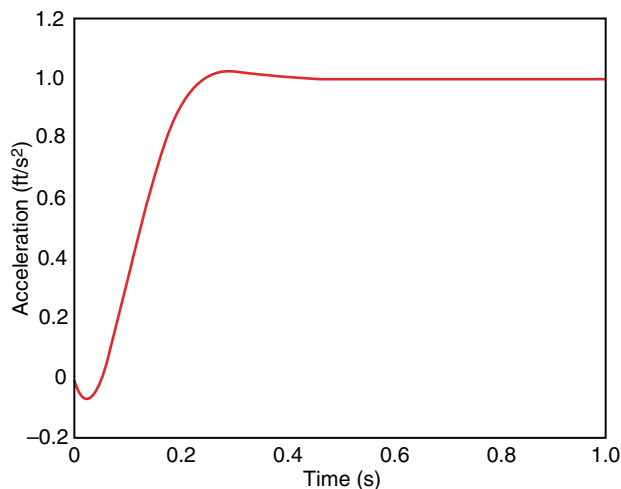


**Figure 14.** The response to a unit-step input acceleration command for the pitch acceleration control system example is shown. This response illustrates the characteristics of a good design, such as a small time constant, small overshoot, and zero steady-state error. The initial acceleration in the negative direction is common to tail-controlled missiles.

tracking the command. This feature is common to tail-controlled missiles. The tail must develop a negative force at the aft end of the missile in order to pitch the nose up and develop a positive AOA. The initial negative kick by the tail moves the center of gravity in the negative direction before the AOA increases and develops positive lift to accelerate the missile in the desired direction.

Figure 15 shows the Bode plot of the open-loop frequency response with the loop broken at the actuator. The gain and phase margins are indicated on the plot and at first glance appear to meet the classical criteria of 6 dB and 30°, respectively. However, the true gain and phase margins might be considerably lower once other effects are included in the model, such as IMU dynamics and measurement latencies as well as time delays associated with the digital implementation of this autopilot in the flight computer. The Bode plot also shows another desirable aspect of a good design: the gain curve is monotonically decreasing at high frequencies, which provides some robustness against unmodeled high-frequency dynamics, such as the aforementioned flexible body vibrations.

## TECHNOLOGY CHALLENGES

In this section, we review the classical approach to designing missile flight control systems and discuss where improvements are needed as the requirements on the flight control system become more stringent to pace the threat.

The classical approach to designing the missile flight control system can be summarized as follows.

1. Develop linear models of the actuator and sensor.
2. Define the functional form of the autopilot equations.
3. Develop a linear model of the missile dynamics at a flight condition of interest.
4. Design autopilot gains in the pitch, yaw, and roll channels, assuming an aerodynamically decoupled airframe to meet basic time-domain requirements.
5. Design additional compensation for aerodynamic cross-coupling.
6. Design additional filters to attenuate sensor noise and flexible body vibrations.
7. Assess linear robustness and performance of the fully coupled system.
8. Return to 4 if necessary.
9. Repeat 3–8 for all flight conditions of interest.
10. Develop a methodology to smoothly transition from one set of gains to the next as the missile flies through different flight conditions.
11. Add nonlinear features, such as actuator command limits, if necessary.

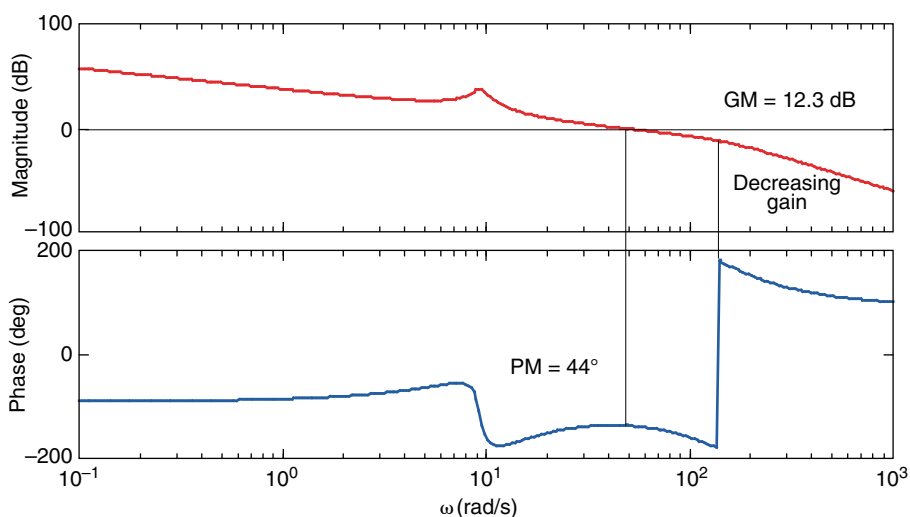


**Figure 15.** The Bode plot with the loop broken at the actuator input for the example pitch acceleration control system shows the characteristics of a good design. The gain is high at low frequency and low at high frequency. The stability margins are high. These margins will be reduced as other effects are included in the analysis, such as IMU dynamics and flight computer processing computational delay.

12. Evaluate in a high-fidelity simulation using nonlinear aerodynamic, actuator, and sensor models.
13. Return to 3 if necessary.

This approach has worked well in the past and will continue to work well in the future for many applications. However, for high-performance interceptors that need to achieve a high AOA with a small time constant, this approach can suffer. One potential problem is the separate steps in 4 and 5 for dealing with the aerodynamic coupling. Intuitively, it might be expected that designing the in-channel and cross-coupling compensation in a unified design approach would yield superior performance. Another area for improvement is the way in which the high-fidelity models are used only for assessment after the basic design is complete. As required time constants decrease, the autopilot will likely saturate the actuator for longer periods of time, suggesting that nonlinear simulation may need to be integral to the design process. Further complicating the design is that steps 3–8 might need to be carried out for thousands of operating conditions.

As the classical design approach evolves, the following challenges need to be addressed:

- The design approach should account for hardware nonlinearities as a fundamental element of the design process.
- The design approach needs to be easily automated so that computer programs can be written to design the autopilot gains over the entire flight envelope to minimize the need for “design by hand.”
- The design approach should work directly on the fully coupled model of the missile dynamics.
- A good design approach should yield a design that is easily adaptable to changes in the missile configuration, specifically the mass properties that tend to change over the course of a missile development and production program.

Though not explicitly stated, any desirable design method should yield a robust control system when properly applied.

The first challenge can be addressed by designing the autopilot using numerical optimization programs. The cost function that is optimized can include many if not all of the FOMs previously discussed, including those from the time-domain response as determined from high-fidelity simulations that include models of the system hardware with their nonlinear dynamics. In this way, the trade-off between robustness and nonlinear time response is brought directly into the process. The challenge then becomes developing a cost function that will meet engineering design goals when it is optimized. The last three challenges can be addressed through the

selection of the specific design method to apply to any particular system. Many control system design techniques are available, but finding one method that meets all three of these criteria is difficult. APL’s contributions in this area are addressed in the next section.

## APL CONTRIBUTIONS

APL has been involved in the development of flight control systems for the Navy since the earliest missiles were being developed. For many of these programs, APL serves as the Technical Direction Agent and, as such, provides support over the life cycle of a missile program. APL also evaluates new theoretical developments in control theory for their applicability to the missile flight control design problem.

### Life Cycle Support

During the concept development phase of a program, APL is involved in developing the requirements for the flight control system. These requirements then flow down to subsystem requirements on the airframe, actuator, and IMU. Typically, this subsystem flow-down requires some level of an autopilot design to demonstrate the feasibility of the entire system meeting the flight control requirements.

As the missile program proceeds to the development phase, APL works closely with the design contractor to ensure a robust design that meets requirements. APL develops models, independent of the contractor, that can be used for model verification and performs an independent assessment of the design. This assessment includes linear analyses as well as predictions from high-fidelity time-domain simulations. Parts of the analyses may replicate those performed by the contractor to verify results. The results of these analyses are communicated back to the contractor with emphasis on areas of concern and potential solutions that may need to be addressed in a subsequent design iteration.

As the program progresses to the test-flight phase, APL works with the contractor and other organizations to develop test objectives and scenarios. The scenarios are designed to maximize coverage over the design space and demonstrate flight control performance, with particular emphasis on the time constant and maximum acceleration. Along with scenario development are pre-flight predictions based on high-fidelity simulations. After the flight, APL again conducts an independent postflight analysis and also uses the flight test data for model validation.

### Technology Development

In addition to supporting missile development programs, APL has taken an active role in applying new

theoretical developments in the field of control systems design and assessing their applicability to the missile flight control design problem. Our particular emphasis has been on addressing the last three challenges listed previously, i.e., developing design methods that can be automated, apply to the fully coupled pitch–yaw–roll dynamic model, and are adaptable to changes in the missile configuration. This activity has been ongoing since the earliest Navy missile programs. This article covers only the relatively recent activities over the last 20 years or so.

In the late 1980s, APL demonstrated that the linear quadratic regulator (LQR) theory can be applied to the missile autopilot design problem. The LQR design problem is to find the control input that minimizes a quadratic function of the state and control

$$C = \int_0^{\infty} (x^T Q x + u^T R u) dt, \quad (20)$$

where  $x$  is the vector of state variables—e.g., AOA, AOS, etc.—and  $u$  is the vector of control inputs—e.g., pitch, yaw, and roll tail deflections. The constant, symmetric weighting matrices,  $Q$  and  $R$ , must be selected to reflect the desired time-domain design criteria, such as time constant and overshoot. The primary benefit of the LQR approach is that the control solution typically has very good stability margins. The difficulty had always been in the appropriate selection of  $Q$  and  $R$  to represent engineering design criteria. APL used the theoretical work of Harvey and Stein,<sup>2</sup> where  $Q$  and  $R$  can be constructed to specify a desired eigenstructure of the closed-loop control system. The closed-loop eigenvalues can be specified based on time-domain requirements, and the eigenvectors can be specified to reflect the desired degree of decoupling between the control channels. This approach has been demonstrated to yield robust designs based on the fully coupled dynamic model and can be automated to work on all flight conditions across the battle space. It does not, however, easily adapt to changes in the missile configuration. Such changes typically require another iteration of the design over the entire design space.

The late 1980s and early 1990s saw an explosion in the use of so-called  $H_{\infty}$  design techniques, primarily as a result of the groundbreaking solution of the control problem indicated in Fig. 16.<sup>3</sup> In the frequency domain, the mathematical objective is to find the controller  $K(s)$  to compute the control  $u$  based on measurements  $y$  from the plant  $P(s)$  that minimizes the infinity norm of the transfer function matrix that relates the inputs  $w$  to the outputs  $z$ . The infinity norm of a transfer function matrix is defined as

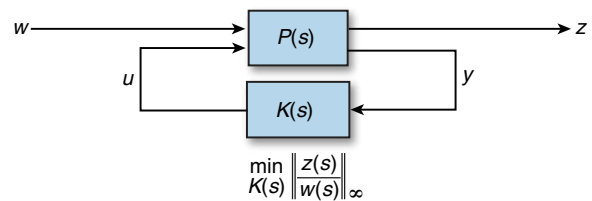


**Figure 16.** The  $H_{\infty}$  design problem is to find the controller  $K(s)$  that minimizes the infinity norm of the transfer function from the inputs in vector  $w$  to the outputs in vector  $z$ . For the flight control design problem, the plant  $P(s)$  models the actuator, airframe, and IMU dynamics. The controller  $K(s)$  is the frequency-domain representation of the autopilot. The inputs  $w$  are the guidance commands and the outputs  $z$  are frequency-weighted signals, such as the achieved acceleration. The frequency-dependent weights can be chosen to represent typical time-domain and frequency-domain design objectives. An approximate solution to this problem can be reached through an iterative approach and involves the solution of two algebraic Riccati equations for each iteration.

$$\|H(s)\|_{\infty} = \sup_{\omega=0 \rightarrow \infty} \bar{\sigma}(H(j\omega)). \quad (21)$$

Loosely speaking, the infinity norm is a measure of the maximum gain from input to output over all frequencies.

For the flight control application, the plant represents the missile dynamics, actuator, and IMU. The controller is the autopilot. The control  $u$  is the actuator command, and the measurements  $y$  are the IMU outputs. The inputs  $w$  would include, for example, pitch and yaw acceleration commands, and the outputs  $z$  would include the pitch and yaw acceleration errors and the missile roll rate. The key is that the outputs are not the actual signals themselves but frequency-weighted versions of those signals. The frequency-dependent weights map time and frequency-domain design goals to the peak gain over all frequencies of the transfer function from  $w$  to  $z$ .

This approach works well for designing missile autopilots at specific operating conditions based on a fully coupled model of the missile dynamics. However, it results in high-order controllers that may be difficult to implement, and it is not easy to automate over the design space. APL pioneered the use of this method for the autopilot design problem. Some of this work is contained in Refs. 4–9.

In the early-to-mid-1990s, APL took the lead on the Highly Responsive Missile Control System Advanced Technology Demonstration program. This program had several objectives, one of which was to demonstrate the efficacy of modern design techniques for the flight control problem and show that the resulting design could be implemented in real time on an embedded processor.

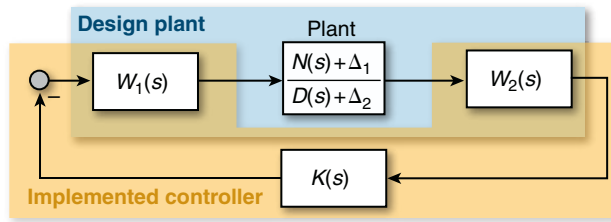


**Figure 17.** The normalized co-prime factorization approach uses frequency-dependent weights to shape the open-loop frequency response. The design problem is to solve for the controller  $K(s)$  to achieve the desired open-loop response and simultaneously maximize robustness to uncertainty in the numerator and denominator of the transfer function that models the plant dynamics. The weights  $W_1(s)$  and  $W_2(s)$  are treated as part of the plant for designing  $K(s)$  and then appended to  $K(s)$  for the controller that is implemented in the missile software.

The design method used in this program was based on the normalized, co-prime factorization (NCF) approach.

In the NCF approach, the plant in the frequency domain is viewed in terms of a transfer function numerator and denominator ( $N(s)$ ,  $D(s)$ ), where each has some associated uncertainty, as in Fig. 17. The control problem is to find the controller  $K(s)$  to achieve the desired open-loop frequency response specified by the weighting functions  $W_1(s)$  and  $W_2(s)$  and simultaneously maximize the size of the uncertainty that would result in an unstable system. The weighting functions are specified by the designer as part of the plant model in the design step and then combined with  $K(s)$  for implementation. Examples using this approach can be found in Ref. 10.

The NCF approach was shown to yield solid, robust designs and could be automated across the design space. However, a completed design does not readily adapt to changes in the missile configuration. Also, it does yield high-order controllers that can be difficult to implement. Unfortunately, the effort was halted before it could be shown that the resulting design could be implemented in real time.

In the mid-1990s, APL was involved in the analysis of various missile system concepts being proposed for the tactical ballistic missile defense mission. To assess these concepts, APL developed weapon system simulations to evaluate predicted performance. Although none of the conceptual systems had actually been designed at this point, the Navy nevertheless desired that the simulations be of relatively high fidelity. To this end, APL had to design prototype flight control systems that could be used in high-fidelity, nonlinear, launch-to-intercept simulations that used fully coupled aerodynamic models. These prototype designs had to be developed reasonably quickly, be easily modified to adapt to weight and center-of-mass changes to each concept, and represent the expected tactical performance of each of these concepts.

To this end, APL used a technique called nonlinear dynamic inversion to quickly design prototype flight control systems. At its core, this technique is very simple, yet it is a powerful design approach. Consider the nonlinear system that is affine in the control input,

$$\dot{x} = f(x) + g(x)u. \quad (22)$$

The control  $u$  is to be designed such that the system dynamics follow some desired trajectory that is a function of the state and commanded state,

$$\dot{x}_d = h(x, x_c). \quad (23)$$

A typical form for the desired dynamics is a first-order lag,

$$h(x, x_c) = \frac{x_c - x}{\tau}, \quad (24)$$

with  $\tau$  being the desired time constant. These desired dynamics can be achieved through a feedback control law of the form

$$u = g^{-1}(x)(h(x, x_c) - f(x)), \quad (25)$$

assuming that the state vector can be measured.

For the acceleration autopilot design problem, for example, the dynamic inversion actually is used twice. First, it is applied to develop control of the missile pitch rate given a desired pitch rate command. Once the pitch rate control loop is designed, it becomes part of the effective plant for which the outer acceleration control loop is defined, using the guidance acceleration command as the reference input.

The dynamic inversion design approach is appealing. It is a simple concept to understand and apply. Because the missile dynamics are explicitly part of the control law, it is easily automated and works directly on the nonlinear, fully coupled pitch–yaw–roll dynamic model. A direct consequence is that the autopilot design naturally adapts to modifications in the missile configuration. For example, a change to the missile mass properties can be naturally accommodated by updating values in the computations of  $f(x)$  and  $g(x)$  in Eq. 25, whereas for the autopilot shown in Fig. 6, the relationship between the values of each gain and the mass properties will not be readily apparent.

The primary drawback of the dynamic inversion approach is that it does not provide any theoretical guarantees of robustness. Instead, it relies on an experienced designer to specify desired dynamics that can be reasonably achieved by the airframe and within the bandwidth constraints of the system hardware. As with any design

approach, the final design must be thoroughly assessed in a high-fidelity simulation and through linear analysis techniques.

Despite this one drawback, the advantages of the dynamic inversion approach make it very appealing. In addition, the desired dynamics could potentially be made a function of time as well, for example, to make the missile more responsive as it approaches intercept at short time-to-go. The implications of a time-varying design on flight control system performance and on missile performance as a whole are as yet unexplored.

## CONCLUSION

This article has covered a variety of topics related to the missile flight control system. The design of this important missile subsystem will continue to evolve to realize the maximum capability of the missile airframe to engage the stressing threats expected in the future.

**ACKNOWLEDGMENTS:** G. A. Harrison and A. P. Iwaskiw of the APL Guidance, Navigation, and Control Group provided several helpful inputs for this article.

## REFERENCES

- <sup>1</sup>Jackson, P. B., "A Gradient Projection Algorithm for Missile Autopilot Stability Analysis," in *Proc. AIAA Guidance, Navigation, and Control Conf.* (1992).
- <sup>2</sup>Harvey, C., and Stein, G., "Quadratic Weights for Asymptotic Regulator Properties," *IEEE Trans. Autom. Control* **AC-23**(3), 378–387 (June 1978).
- <sup>3</sup>Glover, K., and Doyle, J., "State-Space Formulae for All Stabilizing Controllers that Satisfy and H-Infinity Norm Bound and Relations to Risk Sensitivity," *Systems Control Lett.* **11**, 167–172 (1988).
- <sup>4</sup>Reichert, R. T., "Application of H-Infinity Control to Missile Autopilot Designs," in *Proc. AIAA Guidance, Navigation, and Control Conf.* (1989).
- <sup>5</sup>Ruth, M. J., "A Classical Perspective on Application of H-Infinity Control Theory to a Flexible Missile Airframe," in *Proc. AIAA Guidance, Navigation, and Control Conf.* (1989).
- <sup>6</sup>Jackson, P. B., "Applying  $\mu$ -Synthesis to Missile Autopilot Design," in *Proc. 29th IEEE Conf. on Decision and Control*, pp. 2993–2998 (1990).
- <sup>7</sup>Reichert, R. T., "Robust Autopilot Design Using  $\mu$ -Synthesis," in *Proc. American Control Conf.*, pp. 2368–2373 (1990).
- <sup>8</sup>Reichert, R. T., "Dynamic Scheduling of Modern-Robust-Control Autopilot Designs for Missiles," *IEEE Control Systems Magazine* **12**(5), 35–42 (1992).
- <sup>9</sup>Nichols, R. A., Reichert, R. T., and Rugh, W. J., "Gain Scheduling for H-Infinity Controllers: A Flight Control Example," *IEEE Trans. Control Sys. Technol.* **1**(2), 69–79 (1993).
- <sup>10</sup>Iglesias, P. A., and Urban, T. J., "Loop Shaping Design of a Missile Autopilot—Controller Configurations and Weighting Filter Selection," in *Proc. AIAA Guidance, Navigation, and Control Conf.* (1999).

# The Author

**Paul B. Jackson** is a member of APL's Principal Professional Staff and the supervisor of the Aerodynamic Vehicles Section of the Guidance, Navigation, and Control Group in the Air and Missile Defense Department. He graduated from Washington University in St. Louis in 1988 with a B.S. degree in systems science and engineering and received an M.S. degree in electrical engineering from The Johns Hopkins University in 1992. Since joining APL in 1988 as an engineer in the Guidance, Navigation, and Control Group, Mr. Jackson has worked on many aspects of missile guidance and control, including autopilot design, guidance laws, guidance filtering, seeker control, hardware modeling, and simulation development. These activities have spanned a wide variety of programs including Standard Missile-2 Block IIIB, Block IV, and Block IVA; Tomahawk; and Standard Missile-6. His e-mail address is paul.jackson@jhupl.edu.



Paul B. Jackson

The Johns Hopkins APL Technical Digest can be accessed electronically at [www.jhuapl.edu/techdigest](http://www.jhuapl.edu/techdigest).